Reconstructed structures in metal/Si(100) surfaces at high temperature observed by scanning tunneling microscopy

T. Ichinokawa, H. Itoh, A. Schmid, and D. Winau
Department of Applied Physics, Waseda University, 3-4-1, Ohkubo, Shinjuku-ku, Tokyo 169, Japan

J. Kirschner
Max-Planck-Institut fur Mikrostrukturphysik, Weinberg 2, 0-4050 Halle/Saale, Germany

(Received 9 August 1993, accepted 9 February 1994)

Reconstructed structures of metal on Si(100)2×1 surfaces annealed at high temperature have been investigated by scanning tunneling microscopy as functions of the type of metal, coverage, and annealing temperature. The reconstruction mechanisms at high temperature depend on the type of metal. In the present paper, the formation mechanisms of reconstruction at high temperature are classified briefly into three categories and are discussed qualitatively.

I. INTRODUCTION

The surface structures and growth modes in the metal–semiconductor interface have been investigated to make clear the formation mechanisms of reconstructed structures as functions of the type of metal, substrate temperature, and metal coverage. A number of studies by low energy electron diffraction (LEED) and Auger electron spectroscopy (AES) found that there are many superstructures, depending on the coverage and annealing temperature. However, structures determined by LEED and AES are not on the atomic scale. Therefore, the reconstruction mechanisms of superstructures have been investigated by scanning tunneling microscopy (STM) for the high temperature phases in the metal/Si(100) systems. The reconstructed structure of several metals on the Si(100)2×1 surface is analyzed by STM and the mechanisms of reconstruction at high temperature are classified briefly into the three groups depending on the type of metal.

II. EXPERIMENT

Ag(I), Mg(II), Al(III), Pb(IV), Pt(VIII), and Pd(VIII) on the Si(100)2×1 surface were prepared in ultrahigh vacuum (UHV) of 2×10^{-10} Torr and the structures of the deposited surfaces were studied by LEED, AES, and UHV-STM (OMICRON-UHV-STM) as functions of coverage and annealing temperature. The substrate temperature was elevated by electron beam bombardment from back of the specimen and measured by an infrared pyrometer or a thermocouple. All STM images of the prepared samples were taken at room temperature after the samples were transferred from a sample holder of LEED and AES to that of STM by an oblique-stick. The coverages were measured with a quartz thickness monitor and given in monolayers, with 1 ML defined as the Si atom density on the Si(100) surface (1 ML=6.8×10^{14} atoms/cm^2). The local coverage was also estimated by counting the density of metal-related features on the surface seen in the STM images.

III. DIFFERENT TYPES OF RECONSTRUCTED STRUCTURES AT HIGH TEMPERATURE

Besides Pb, the surface structures deposited at low temperature transform into high temperature phases by reconstruction at coverages less than 1 ML. The reconstruction mechanisms are classified into the following three categories on the basis of the structures observed by STM.

A. Long range ordering of Si-missing dimer defects combined with adsorbed metal atoms

For depositions of Pt (Ref. 1) and Pd (Ref. 2) at room temperature, clusters of nm size nucleate in the Volmer–Weber (V–W) mode. Therefore, a LEED pattern of the Si(100)2×1 structure becomes obscure with increasing coverage and disappears at a thickness of several monolayers. However, by annealing up to 800 °C the sharp LEED patterns of $c(4\times2)$ and $c(4\times6)$ appear in a range from 1/6 or 1/3 ML. A STM image of the mixed structure of $c(4\times2)$ and $c(4\times6)$ is shown in Fig. 1 with their model. In the STM image of Fig. 1(a), we can observe two kinds of protrusions; one is gray in a square shape and the other is bright in an oval shape. The gray protrusions of the square shape form a $c(4\times2)$ structure and the bright protrusions of the oval shape form a $c(4\times6)$ structure. From the STM image, it can be suggested that $c(4\times2)$ consists of subunits composed of two-dimers and an embedded Pd (or Pt) atom at the center and $c(4\times6)$ consists of subunits in which a Si dimer is missing from the $c(4\times2)$ subunit.

In the Si(100) clean surface, a number of Si-missing dimer clusters exist and they are dispersed into individual missing dimer defects by metal adsorption and annealing combining with a metal atom. The subunit of a Si-dimer combined with an adsorbed metal atom forms a regular $c(4\times6)$ superstructure as shown in Fig. 1(b). The reconstructed structure of $c(4\times2)+c(4\times6)$ covers all over the surface at 1/3 ML and above 800 °C and is stable from room temperature to desorption temperature after the formation of the reconstructed structure. Beyond the coverage of the reconstruction, three-dimensional (3D) islands nucleate on this surface in the Stranski–Krastanov (S–K) mode as shown in Fig. 2 and the composition of islands is silicide from another experiment of micro-AES.

The similar formation of the reconstructed structures to that of the Pt and Pd/Si(100) systems was reported in a Ni-contaminated surface of Si(100). The ordered structure of Si-missing dimer defects is induced by a Ni impurity; i.e.,

 0734-211X/94/12(3)/2070/4/$1.00

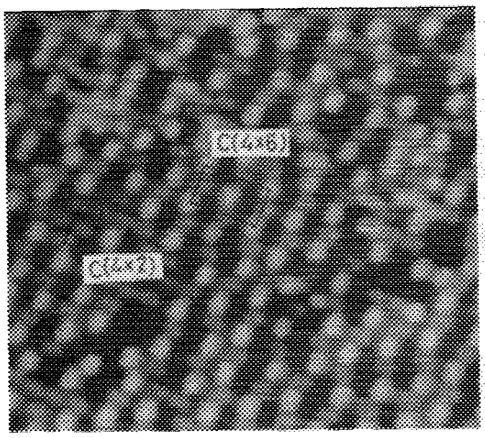

(a)

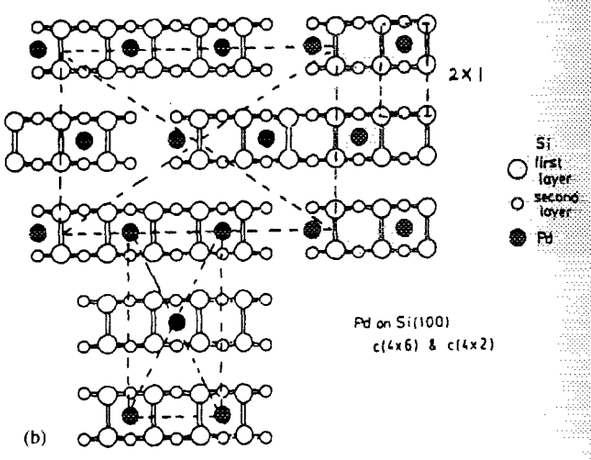

(b)

FIG. 1. (a) A STM image of the $c(4\times2)+c(4\times6)$ surface and (b) model of the $c(4\times2)+c(4\times6)$. $c(4\times2)$ is composed of a subunit which consists of two dimers and a Pd atom embedded at the center, and $c(4\times6)$ consists of a subunit in which a Si dimer is missing from the $c(4\times2)$ subunit.

the $2\times n$ structure ($2<n<10$) has been observed, where n depends on the Ni-coverage in the surface. The structure analyses of this surface were already performed by LEED[3,4] and STM.[5]

B. Long range ordering of metal molecular clusters consisting of several atoms

The Al deposited surface on the Si(100)2×1 surface at coverages less than 0.5 ML and temperature lower than 350 °C has 2×2, 2×3, and 2×5 structures depending on an interline spacing between Al-dimer lines perpendicular to the underlying Si-dimer rows. The topmost layer of the 2×2 structure is completed at 0.5 ML, and 3D islands nucleate at above 0.5 ML on this surface in the S–K mode.

However, by annealing up to 500 °C the LEED pattern changes from 2×2 to $c(4\times12)$ as reported by Ide *et al.*[6] The STM image of the reconstructed structure observed at 500 °C and a coverage of 0.2 ML is shown in Fig. 3. Although the structure of Fig. 3 has a number of imperfections, a $c(4\times12)$ unit mesh is observed as shown by a rectangle. A bright protrusion is not a single atom but is a metal molecule with a hexagonal symmetry as shown by a magnified image of the insert (A). The neighboring Si-dimer rows buckle with out-of-phase due to the chemisorption of metal molecules. The Al molecules form superstructures of $c(4\times2n)$ due to the buckling of the Si-dimer rows. From a nominal Al coverage determined by AES, we can estimate that a molecular consists of 6 ± 1 Al atoms. The model of the $c(4\times12)$ superstructure is illustrated in Fig. 4. Furthermore, in Fig. 3 we can see the formation of layer islands of 2×1 and 2×2 structures on the $c(4\times2n)$ surface. The layer islands of 2×1 and 2×2 illustrated in the inserts (B) and (C) are 2D Si and Al islands, respectively, formed by destruction of the underlying Si dimer structure. The formation of the Si(100)$c(4\times12)$-Al phase is induced by metal molecules and buckling of the underlying Si-dimer rows with out-of-phase.

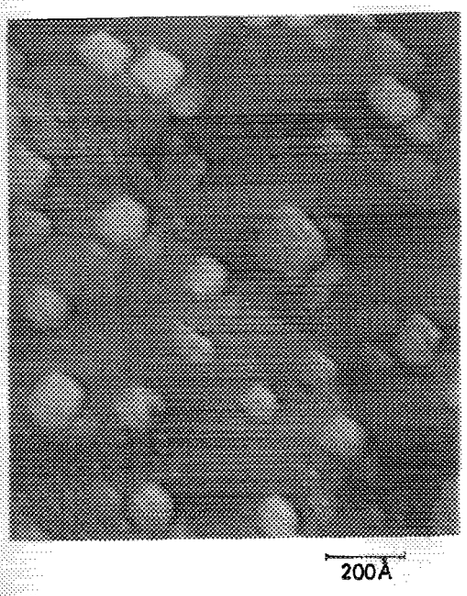

FIG. 2. A STM image of the Pt/Si(100) surface at a Pt thickness of 15 Å and an annealing temperature of 800 °C. The clusters are 20 Å thick and silicide.

The reconstruction similar to that of the Al/Si(100) phase at high temperature was reported by Baski, Nogami, and Quate[7,8] for the deposited surfaces of III-group metals (In and Ga) on Si(100) and for a Ni-contaminated Si(111) surface of $\sqrt{19}\times\sqrt{19}$ by Wilson and Chiang[9] from STM observations.

C. Formation of optimized structure in metal and Si interface

For several metals, superstructures of the chemisorbed state at high temperature are formed without any relation to the Si missing dimer defects or formation of the metal molecules described in the previous sections. The reconstruction is determined by the optimized structure between metal and Si substrate.

For instance, Ag forms a 2×3 structure as shown in Fig. 5 at above 500 °C (Ref. 10) and Mg forms 2×3 and 2×2 struc-

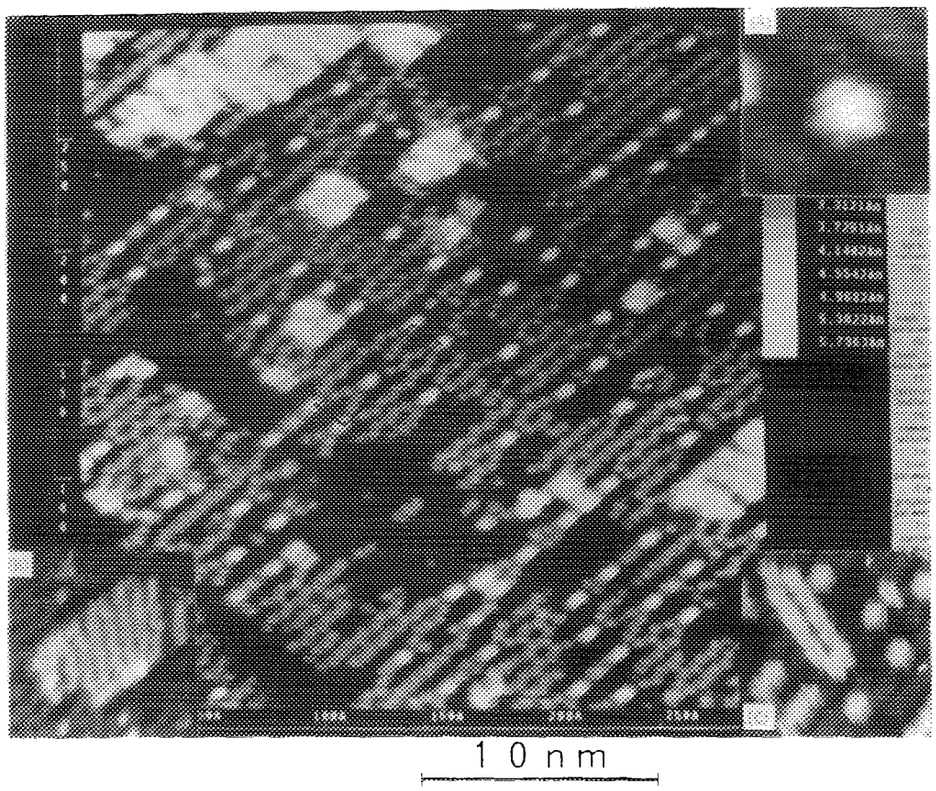

FIG. 3. A STM image for the Al deposited surface of 0.2 ML at 500 °C. The bright protrusions form the $c(4\times 2n)$ structure as shown by a rectangle. The magnified image of a molecular cluster has a hexagonal symmetry as shown by an insert (A). Two types of layer islands with structures of 1×2 and 2×2 are Si and Al formed in the second layer as shown by the insert (B) and (C), respectively.

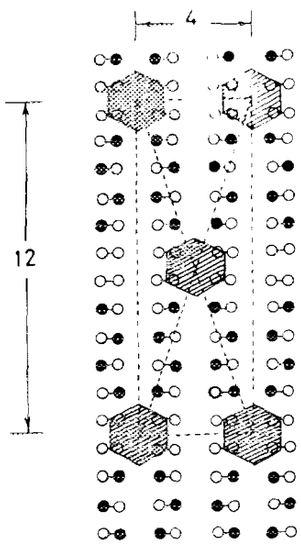

FIG. 4. The model of the structure of Al/Si(100)-$c(4\times 12)$.

tures depending on the coverage at above 500 °C. These structures are formed by minimization of surface energy for metal chemisorbed surfaces on Si(100)2×1. The magnified STM images of the Si(100)2×3-Ag surface is shown in Fig. 6 together with its structure model. From the STM images taken at various bias voltages, we determine that Ag atoms align in the groove at the bridge site between adjacent Si-

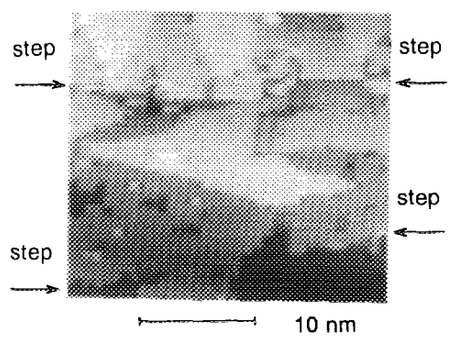

FIG. 5. The Si(100)2×1 surface covered with 0.15 ML Ag at 500 °C. The Si dimer rows are visible on the terraces and Ag atoms form 2D islands of the 2×3 structure with triangular shapes. The Ag rows run along the parallel lines between Si-dimer rows.

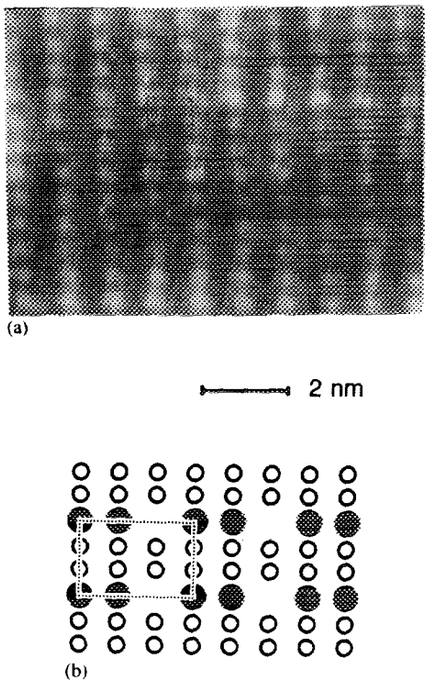

FIG. 6. (a) A STM image of the 2×3 structure. (b) Model of the 2×3 structure, where the small open circles denote the Si dimer atoms and the full circles Ag atoms.

dimers and every third atom is missed along the Ag line.

The 2D islands of 2×3 with triangular shapes in Fig. 5 cover all of the surface at 0.3 ML, and 3D islands nucleate above 0.3 ML in the S–K mode on the completed surface of 2×3. This type of reconstruction is the most popular even in the metal–Si interface, although several modifications exist in growth mode.

IV. DISCUSSION

In the several metal/Si(100)2×1 surfaces, the three types of reconstruction have been found at high temperature. The different mechanisms of reconstruction are caused by difference of the surface energy depending on the reconstructed structures. The 3D phase diagrams of metal–Si binary alloys are explained thermodynamically under the condition of minimum free energy, taking account of the interaction between metal–metal and metal–Si bonds. For the 2D phase diagrams, however, we have to calculate the total surface energy for the reconstructed structures. Therefore, 2D reconstructed structures are more complicated than those of 3D phases and it is very difficult to suggest the reconstructed structures beforehand.

So far the studies on an early stage of epitaxial growth in the metal on Si surfaces have been reported for various metals, however, the difference of formation has not been discussed as a function of the type of metal. The metals in a same group of the Periodic Table form superstructures by means of a similar mechanism. However, the surface structures depend on the total surface energy of binary alloy systems. As a result, intermixing between metal and Si or displacement of Si atoms from substrate to toplayer occur often in the interface and reconstruction also depends on the surface planes of Si substrate. Consistent discussions on the formation of reconstructed structures in metal on Si systems could be performed after the systematic analyses for various types of reconstruction.

V. CONCLUSION

Reconstructed structures of metal on Si(100)2×1 systems have been investigated by STM as a function of the type of metal. The reconstructions at high temperature depend on the type of metal and are classified nominally into three groups in this paper from their formation mechanisms. The systematic analyses for different types of reconstruction depending on the type of metal will be helpful in gaining knowledge on reconstruction mechanisms.

ACKNOWLEDGMENT

The present work was supported by a Grant-in-Aid for Scientific Research and Culture from the Japanese Ministry of Education.

[1] H. Itoh, S. Narui, A. Sagawa, and T. Ichinokawa, Phys. Rev. B **45**, 11136 (1992).
[2] H. Itoh, S. Narui, H. Tanabe, and T. Ichinokawa, Surf. Sci. **284**, 236 (1993).
[3] K. Kato, T. Ide, S. Miura, A. Tanabe, and T. Ichinokawa, Surf. Sci. **194**, L87 (1988).
[4] J. A. Martin, D. E. Savage, W. Moritz, and M. G. Lagally, Phys. Rev. Lett. **56**, 1936 (1986).
[5] H. Niehus, U. K. Koler, M. Copel, and J. E. Demuth, *Proceedings of the 3rd International Conference on STM, Oxford, 1988*, Vol. 23 Suppl. 3 (Royal Microscopical Society, London, 1989), p. 13.
[6] T. Ide, T. Nishimori, and T. Ichinokawa, Surf. Sci. **208**, 335 (1989).
[7] A. A. Baski, J. Nogami, and C. F. Quate, J. Vac. Sci. Technol. A **9**, 1946 (1991).
[8] A. A. Baski, J. Nogami, and C. F. Quate, Phys. Rev. B **43**, 9316 (1991).
[9] R. J. Wilson and S. Chiang, Phys. Rev. Lett. **58**, 2575 (1987).
[10] D. Winau, H. Itoh, A. K. Schmid, and T. Ichinokawa, Surf. Sci. **303**, 139 (1994).